Am J Physiol Renal Physiol 282: F730–F740, 2002.
First published November 20, 2001; 10.1152/ajprenal.00298.2001.

Acute hypertension provokes internalization of proximal tubule NHE3 without inhibition of transport activity

LI YANG,[1] PATRICK K. K. LEONG,[1] JENNIFER O. CHEN,[1] NILEM PATEL,[1] SARAH F. HAMM-ALVAREZ,[1,2] AND ALICIA A. MCDONOUGH[1]
[1]*Department of Physiology and Biophysics, University of Southern California Keck School of Medicine, and* [2]*Department of Pharmaceutical Sciences, University of Southern California School of Pharmacy, Los Angeles, California 90089-9142*

Received 21 September 2001; accepted in final form 13 November 2001

Yang, Li, Patrick K. K. Leong, Jennifer O. Chen, Nilem Patel, Sarah F. Hamm-Alvarez, and Alicia A. McDonough. Acute hypertension provokes internalization of proximal tubule NHE3 without inhibition of transport activity. *Am J Physiol Renal Physiol* 282: F730–F740, 2002. First published November 20, 2001; 10.1152/ajprenal.00298.2001.—Acute hypertension rapidly decreases proximal tubule (PT) Na^+ reabsorption, facilitated by a redistribution of PT Na^+/H^+ exchangers (NHE3) out of the apical brush border, increasing NaCl at the macula densa, the signal for autoregulation of renal blood flow and GFR. This study aimed to determine whether NHE3 activity per transporter decreases during acute hypertension and the time dependence of the response. Blood pressure was elevated by 50–60 mmHg in male Sprague-Dawley rats for 5 or 30 min by constricting arteries. Renal cortical membranes were fractionated by density gradient centrifugation. NHE3 transport activity was assayed as the rate of appearance of acridine orange (AO) from AO-loaded vesicles in response to an inwardly directed Na^+ gradient. After 5-min hypertension, 20% of total NHE3 protein, assayed by immunoblot, redistributed from low-density apical membranes to middensity membranes enriched in intermicrovillar cleft markers; by 30 min, a similar percentage shifted to heavier density membranes containing markers of endosomes. NHE3 activity shifted to higher density membranes along with NHE3 protein, that is, no change in activity/transporter during acute hypertension. Confocal analysis of NHE3 distribution also verified removal from apical microvilli and appearance in subapical vesicles. We conclude that the decrease in renal PT Na^+ transport during acute hypertension is mediated by removal of transport-competent NHE3 from the apical brush border to subapical and internal reserves.

kidney; acridine orange; tubuloglomerular feedback; sodium transport; blood pressure; sodium-hydrogen exchanger

TUBULOGLOMERULAR FEEDBACK (TGF)-driven autoregulation of renal blood flow (RBF) and glomerular filtration rate (GFR) during a rise in blood pressure is initiated by an increase in NaCl delivery to the macula densa. This ionic error signal leads to a cascade of events culminating in increased afferent arteriolar resistance to normalize RBF and GFR and pressure diuresis (5). The increase in NaCl delivery is the consequence of a rapid inhibition of proximal tubule Na^+ reabsorption during acute hypertension (9, 33). We have focused on determining the molecular events that connect a change in blood pressure to the error signal that drives TGF. Active sodium reabsorption across the proximal tubule is mediated by apical entry of Na^+, primarily via NHE3, and basolateral extrusion via sodium pumps (Na,K-ATPase). Our initial studies demonstrated that 5- to 30-min acute hypertension provoked a rapid redistribution of Na^+/H^+ exchanger (NHE3) and Na^+/P_i cotransporter (NaPi), along with megalin and dipeptidyl-peptidase IV (DPPIV), out of the peripheral brush border to the intermicrovillar cleft region and subapical endosomes as well as inhibition of basolateral Na,K-ATPase activity (21, 30, 32, 33). We observed a similar internalization of NHE3 and NaPi and inhibition of Na,K-ATPase in renal cortex after in vivo treatment with PTH and showed that the apical transporter redistribution, but not the Na,K-ATPase inhibition, was dependent on generation of cAMP/protein kinase A (PKA) (34).

The present study aimed to determine whether there were other key cellular mechanisms contributing to the decrease in proximal tubule sodium transport during acute hypertension. Three general mechanisms could explain a rapid inhibition of sodium transport during acute hypertension: *1*) modification of sodium transporters or their regulatory proteins, as illustrated by the ability of NHERF to inhibit NHE3 activity after cAMP elevation in reconstituted systems and cultured cells (27); *2*) removal of sodium transporters from the plasma membrane to intracellular stores, as illustrated by the effect of acute hypertension on NHE3 (30, 32, 33) or the effect of protein kinase C (PKC) stimulation on Na,K-ATPase (8); and *3*) degradation of transporters illustrated by the in vivo effects of high dietary P_i or parathryroid hormone (PTH) treatment on apical NaPi in the proximal tubule (19). In this study, we addressed these possibilities by determining the time

Address for reprint requests and other correspondence: A. A. McDonough, Dept. of Physiology and Biophysics, Univ. of Southern California Keck School of Medicine, 1333 San Pablo St., Los Angeles, CA 90089-9142 (email: mcdonoug@hsc.usc.edu).

The costs of publication of this article were defrayed in part by the payment of page charges. The article must therefore be hereby marked "*advertisement*" in accordance with 18 U.S.C. Section 1734 solely to indicate this fact.

dependency of the internalization response during acute hypertension and testing whether there was an accompanying decrease in Na^+/H^+ exchanger activity per transporter, that is, whether NHE3 removed from the apical microvilli was inactivated, and by determining whether there was increased degradation of NHE3 during induced hypertension. The results indicate that during hypertension there is rapid removal of transport-competent NHE3 from the apical membrane in a two-stage process and that there is no evidence for increased degradation.

EXPERIMENTAL PROCEDURES

Animal preparation. Experiments were performed on male Sprague-Dawley rats (300–350 g body wt) that had free access to food and water before the experiment. Rats were anesthetized intramuscularly with ketamine (Fort Dodge Laboratories) and xylazine (Miles; 1:1, vol/vol) and then placed on a thermostatically controlled warming table to maintain body temperature at 37°C. A polyethylene catheter was placed into the carotid artery to monitor blood pressure. The jugular vein was cannulated to infuse 4.0% BSA in 0.9% NaCl at 50 μl/min throughout the entire experimental period to maintain euvolemia. The ureter was cannulated to collect urine. Mean arterial pressure was increased 50–60 mmHg over basal level by constricting the superior mesenteric artery, celiac artery, and abdominal aorta below the renal artery by tying the silk ligatures around the vessels, as reported previously (32). Three groups of rats (n = 4 each) were compared: *1*) control sham operated, *2*) 5-min acute systolic hypertension and *3*) 30-min acute systolic hypertension.

Homogenization and subcellular fractionation. The procedure for subcellular fractionation of the renal cortex membranes has been described in detail previously (32, 33). In brief, kidneys were cooled in situ by flushing with cold PBS and then excised. The renal cortices were rapidly dissected and homogenized in 5% sorbitol, 0.5 mM disodium EDTA, 0.2 mM phenylmethylsulfonyl fluoride, 9 μg/ml aprotinin, and 5 mM histidine-imidazole buffer, pH 7.5, with a Tissuemizer (Tekmar Instruments) for 10 min at a thyristor setting of 45; they were then centrifuged at 2,000 *g* for 10 min, the pellet was homogenized and centrifuged again, and the low-speed supernatants (S_o) were pooled, loaded at the interface between two hyperbolic sorbitol gradients (ranging between 35 and 70% sorbitol), and centrifuged in a swinging bucket rotor (100,000 *g* for 5 h). Twelve fractions were collected from the top, diluted with isolation buffer, pelleted by centrifugation (250,000 *g* for 1.5 h), resuspended in 1 ml of isolation buffer, and stored at −80°C, pending assays.

Na^+/H^+ exchanger transport activity measurements. Na^+/H^+ exchange activity was measured as reappearance of acridine orange (AO) from loaded vesicles as illustrated in Fig. 1. AO is a weak base (pK = 10.45), with characteristic spectra (excitation = 493 nm and emission = 520 nm), and can be used to monitor changes in transmembrane pH (ΔpH) (25, 29). Transport activity was assessed in either vesicles made from the total membrane S_o fraction or membranes collected from the density gradient. Membranes were diluted into 6 ml of loading solution [(in mM) 150 Na-gluconate, 100 K-gluconate, 1 Mg-gluconate and 10 Tris-HEPES, pH 7.0], pelleted at 250,000 *g* for 60 min, and resuspended into a small volume of loading solution. The protein concentration was measured (20) and adjusted to 25 mg/ml for S_o membranes and 10 mg/ml for membranes from the density gradient. The vesicular suspensions were incubated at 25°C for 2 h before assay. A 10-μl aliquot of membrane suspension was added to a cuvette containing 2 ml of 6 μM AO reaction medium (in mM) 150 *N*-methylglucamine gluconate (NMG-gluconate), 100 K-gluconate, 1 Mg-gluconate and 10 Tris-HEPES, pH 7.0] in the presence of 1 μM valinomycin, and immediately mixed with a cuvette mixer. The change in fluorescence was monitored with a Perkin-Elmer LS5 spectrofluorometer. The amount of AO trapped as AOH in the vesicles, where the signal is quenched, is a function of the H^+ influx via the Na^+/H^+ exchanger (Fig. 1*A*, *left*). After 1 min, Na-gluconate was added to the cuvette to a final concentration of 25 mM, which created an inward-directed Na^+ gradient to drive H^+ efflux via the Na^+/H^+ exchanger, which also drove the intravesicular conversion of AOH to AO and AO efflux or reappearance into external buffer (Fig. 1*A*, *right*). The rate of Na^+/H^+ exchange was calculated from the slope of the initial 2.5-s recovery of AO fluorescence in external

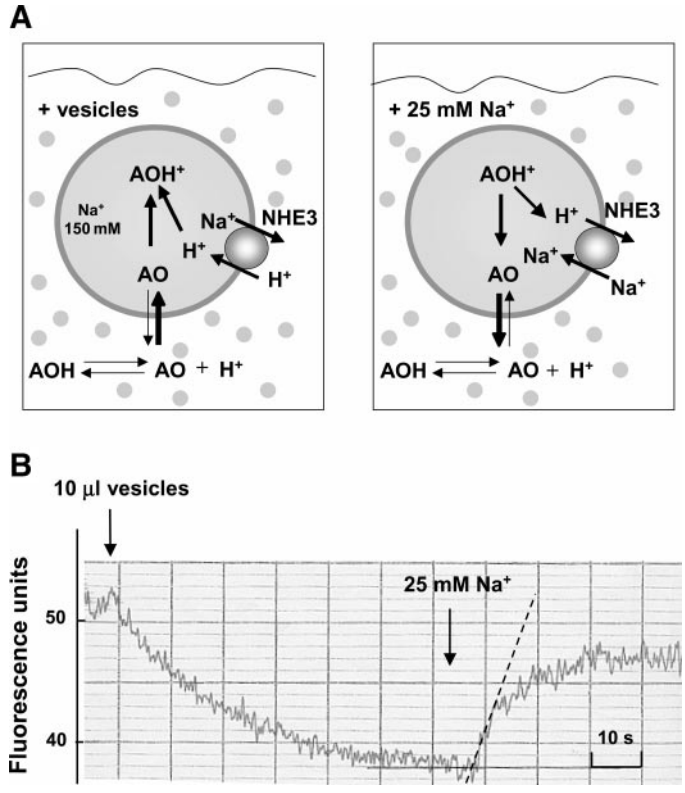

Fig. 1. Na^+-dependent acridine orange (AO) fluorescence quenching and recovery. *A*: AO uptake into and exit from membrane vesicles. The vesicles were preloaded with a solution containing (in mM) 150 Na-gluconate, 100 K-gluconate, 1 Mg-gluconate and 10 Tris-HEPES, pH 7.0. *Left*: a 10-μl aliquot of membrane suspension was added to a cuvette containing 2 ml of 6 μM AO reaction medium [same as loading solution with *N*-methylglucamine gluconate (NMG) replacing sodium] in the presence of 1 μM valinomycin. The amount of AO trapped in the vesicles as AOH is a function of the amount of H^+ influx coupled to the Na^+ efflux via the Na^+/H^+ exchanger. The internal dye is quenched and not detected by spectrofluorometer (*B*). *Right*: after steady-state AO quenching was achieved, 50 μl of 1 M Na-gluconate was added to the external buffer to rapidly reverse the direction of Na^+/H^+ exchange, which drives Na^+ influx coupled to H^+ efflux along with the conversion of AOH to AO and AO efflux into external buffer (*B*). *B*: AO fluorescence tracing. The rate of Na^+/H^+ exchange is calculated from the slope of the initial 2.5-s recovery of AO fluorescence in the external buffer and expressed in arbitrary fluorescence units per second per milligram protein.

buffer, expressed in arbitrary fluorescence units per second per milligram protein (Fig. 1*B*). Quadruplicate measurements of the initial rate of AO fluorescence recovery were made for each sample. Preliminary experiments determined the linear range for protein addition (not shown).

Immunoblot analysis and antibodies. To determine the time dependence of NHE3 redistribution, a constant volume of sample from each gradient fraction was assayed. In the assays of NHE3 activity per transporter, a constant amount of gradient fraction protein, rather than volume, was assayed. In both cases, samples were denatured in SDS-PAGE sample buffer for 30 min at 37°C, resolved on 7.5% SDS-polyacrylmide gels according to Laemmli (18) and transferred to polyvinylidene difluoride membranes (Millipore Immobilon-P). Blots were probed with either polyclonal anti-rat NHE3 L546, generously provided by Dr. M. Knepper (National Institutes of Health) (14), or an analogous polyclonal NHE3-C00 made in this laboratory, both used at 1:1,000 dilution. In one study, we compared antibody detection using L546 with detection using the antibody we have employed in our previous studies: monoclonal antibody 2B9 generously provided by Dr. D. Biemesderfer (Yale University) (2, 32, 34). All blots were detected with an enhanced chemiluminescence kit (Amersham Pharmacia Biotech), and autoradiographic signals were quantified with a Bio-Rad imaging densitometer with Molecular Analyst software. Selected samples on each blot were run at one-half the volume or protein to ensure that the sample was in the linear range of detection, and multiple exposures of autoradiograms were analyzed to ensure that signals were within the linear range of the film. Additional antibodies used to characterize membrane populations included polyclonal antisera to dipeptidyl-aminopeptidase IV (DPPIV) and megalin provided by Dr. M. Farquhar (University of California at San Diego), and rab 5a obtained from Santa Cruz Biotechnology (Santa Cruz, CA).

Indirect immunofluorescence. Kidneys from rats with or without acute hypertension challenge were fixed in situ by placing the isolated kidney in a small Plexiglas cup and bathing it in fixative (2% paraformaldehyde, 75 mM lysine, and 10 mM Na-periodate, pH 7.4; PLP) for 20 min. The kidneys were then removed and cut in half on a midsagittal plane and postfixed in PLP for another 4–6 h. The fixed tissue was rinsed twice with PBS, cryoprotected by incubation overnight in 30% sucrose in PBS, embedded in Tissue-Tek OCT Compound (Sakura Finetek, Torrance, CA) and frozen in liquid nitrogen. Cryosections (5 μM) were cut using a Microm Heidelgerg ultramicrotome, transferred to Fisher Superfrost Plus-charged glass slides, and air dried. For immunofluorescence labeling, the sections were rehydrated in PBS for 10 min, followed by washing with 50 mM NH_4Cl in PBS for 10 min, then with 1% SDS in PBS for 4 min for antigen retrieval (6). SDS was removed by two 5-min washes in PBS; then sections were blocked with 1% BSA in PBS to reduce background. Double labeling was performed by incubating with polyclonal antiserum NHE3-C00 and monoclonal antibody against villin (Immunotech, Chicago, IL), both at a dilution of 1:100 in 1% BSA in PBS for 1.5 h at room temperature. After 5-min washes three times in PBS, the sections were incubated with a mixture of FITC-conjugated goat anti-rabbit and Alexa 568-conjugated goat anti-mouse secondary antibodies (Accurate Chemical & Scientific, Westbury, NY) diluted 1:100 in 1% BSA in PBS for 1 h, washed three times with PBS, mounted in Prolong Antifade (Molecular Probes, Eugene, OR), and dried overnight at room temperature. Slides were viewed using a Nikon PCM Quantitative Measuring High-Performance Confocal System equipped with filters for both FITC and tetramethyl rhodamine isothiocyanate fluorescence attached to a Nikon TE300 Quantum upright microscope. Images were acquired with Simple PCI C-imaging hardware and quantitative measuring software and processed with Adobe Photoshop 5.0 (Adobe Systems, Mountain View, CA).

RESULTS

Characteristics of subcellular membrane pools. Subcellular fractionation of total membranes from whole cortex was conducted to recover 100% of NHE3. Therefore, all cell membranes are resolved in the sorbitol gradient. Characteristics of the 12 fractions collected from the sorbitol density gradients have been reported previously (32, 33). In this study, we simplified the analysis by pooling the gradient fractions into three "windows" on the basis of the previously reported distribution of subcellular membrane markers (32, 33). We focus on NHE3 regulation and redistribution in this study and thus on the distribution of markers useful to describe the NHE3 trafficking pathways. Figure 2 summarizes the characteristics of these windows. *Window I* (*WI*) from *fractions 3–5*, is enriched in apical brush-border markers alkaline phosphatase, DPPIV and NHE3 (see Fig. 5). *Window II* (*WII*), from *fractions*

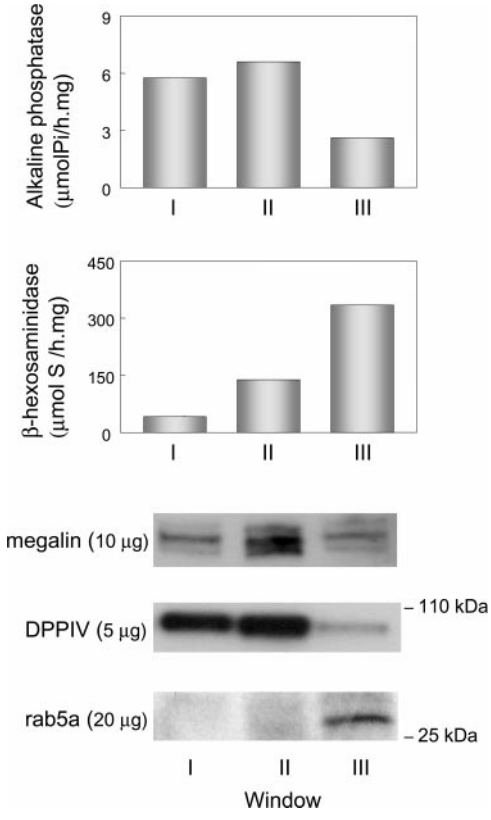

Fig. 2. Characteristics of 3 pools of membranes. Renal cortex density gradient fractions were pooled into 3 windows: *window I*, *fractions 3–5*; *window II*, *fractions 6–8; window III*, *fractions 9–11*. The windows were analyzed for membrane markers by enzymatic assay or Western blot: alkaline phosphatase, an apical membrane marker; β-hexosaminidase, a lysosomal/endosomal marker; megalin, an intermicrovillar cleft marker; dipeptidyl peptidase IV (DPPIV), an apical membrane marker at 105 kDa; and rab 5a, an endosomal protein at 27 kDa.

6–8, contains most of the intermicrovillar cleft marker megalin [gp330, also found in microvilli and subapical endosomes (3)]and the apical markers alkaline phosphatase, DPPIV, and NHE3 (Fig. 5). *Window III* (*WIII*), from *fractions 9–11*, is enriched in the endosomal marker rab 5a (7) and the lysosomal marker β-hexosaminidase. These marker assays confirm the following membrane assignment: *WI* contains apical membranes, *WII* contains a mixed pool of apical and intermicrovillar cleft membranes, and *WIII* contains endosomal and lysosomal pools. From previous work from our laboratory (32–34), we know that *WI* also contains Na,K-ATPase-enriched basolateral membranes, but these membranes do not impact the NHE3 distribution or measurement of activity.

Antibody-specific detection of NHE3. NHE is the major route for apical sodium entry across the proximal tubule, and NHE3 is responsible for virtually all the Na^+/H^+ exchange activity in this region (1, 4). Our previous studies establishing that acute hypertension provokes a rapid redistribution of NHE3 immunoreactivity from lower- to higher-density membranes used two different NHE3 antibodies with slightly different results (32, 33). A polyclonal directed to the rat NHE3 sequence amino acids 687–696 detected a shift out of *WI* into *WIII* (33); this reagent is no longer available. A monoclonal raised to the COOH-terminal 131 amino acids of rabbit NHE3 (2B9) detected a shift out of *WI* primarily into *WII* (not *WIII*) (32). In the present study, we reexamined NHE3 distribution in this gradient with a polyclonal antiserum made to the COOH-terminal 21 amino acids of rat NHE3 (L546) and compared the results to those with 2B9. Figure 3*A* shows representative NHE3 immunoblots, and Fig. 3*B* summaries from sets of control and 30-min hypertension-exposed animals probed in parallel with 2B9 or L546. L546 detects a greater fraction of NHE3 in *fractions 4* and *8* at baseline than 2B9. After 30-min hypertension, ~25% of the NHE3 is seen to shift out of *WI* with either 2B9 or L546, but with L546 a greater fraction moves into *WIII*. These results demonstrate that NHE3 detection is dependent on the antibody used, even under denaturing conditions: both antibodies detect NHE3 in apical brush border and intermicrovillar clefts and detect the shift out of *WI* during hypertension, but L546 detects NHE3 in *WIII*, enriched in endosomes. Distribution of NHE3 with these two antibodies has been assessed by immunocytochemistry under nondenaturing conditions with a similar conclusion: L546 was better at detecting NHE3 in intermicrovillar cleft and subapical pools than 2B9, which stains the villi (2).

Physiological responses. Figure 4 summarizes the effects of constricting arteries for 5 or 30 min on blood pressure, urine output, and endogenous lithium clearance (C_{Li}). Arterial pressure increased immediately by 50–60 mmHg above control level and was maintained for 30 min. Urine output increased 9.23 ± 0.7-fold after 5 min, and the diuresis was maintained during 30-min hypertension. C_{Li^+}, a measure of the volume flow out of the proximal tubule (28), increased about fivefold after 5 min and tended to fall to about threefold over control

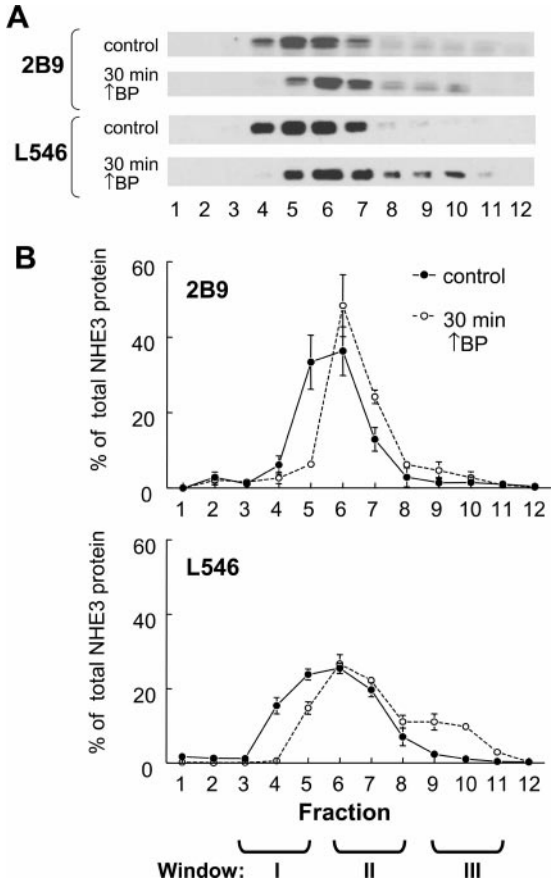

Fig. 3. Comparison of Na^+/H^+ exchanger (NHE3) density distribution patterns with 2 different anti-NHE3 antibodies. *A*: NHE3 was assayed in membrane fractions of renal cortex from control vs. rats after 30-min hypertension (↑BP), where BP is blood pressure. Immunoblots of a constant volume of each fraction from a typical experiment are shown. Duplicate blots were probed with either monoclonal 2B9 or polyclonal L546. *B*: summary of 3 independent experiments comparing duplicate blots probed with 2B9 (*top*) vs. L546 antibody (*bottom*). NHE3 immunoreactivity in each fraction is expressed as the percentage of total signal in all 12 fractions. Values are means ± SE; $n = 3$ rats in control and hypertension groups.

after 30-min hypertension. The magnitude of the increase in blood pressure imposed is within the reported autoregulatory range for GFR and RBF (9, 10); however, we have recently measured (using FITC-inulin clearance) a transient increase, then normalization, of GFR over the first 15 min, which could contribute to this fall in C_{Li^+} (not shown). The elevation of urine output and endogenous lithium clearance during 30-min hypertension indicates that the signals driving the Na^+ transporter response persist during this time period.

Time dependence of NHE3 redistribution. On the basis of the results with L546, we generated another polyclonal antiserum, NHE3-C00, to the same peptide sequence and found it detected NHE3 in gradient fractions ± acute hypertension with the same patterns as L546 (not shown); NHE3-C00 was used for the time course analysis and for immunocytochemistry. To determine the relationship between duration of acute hypertension and the magnitude of redistribution of

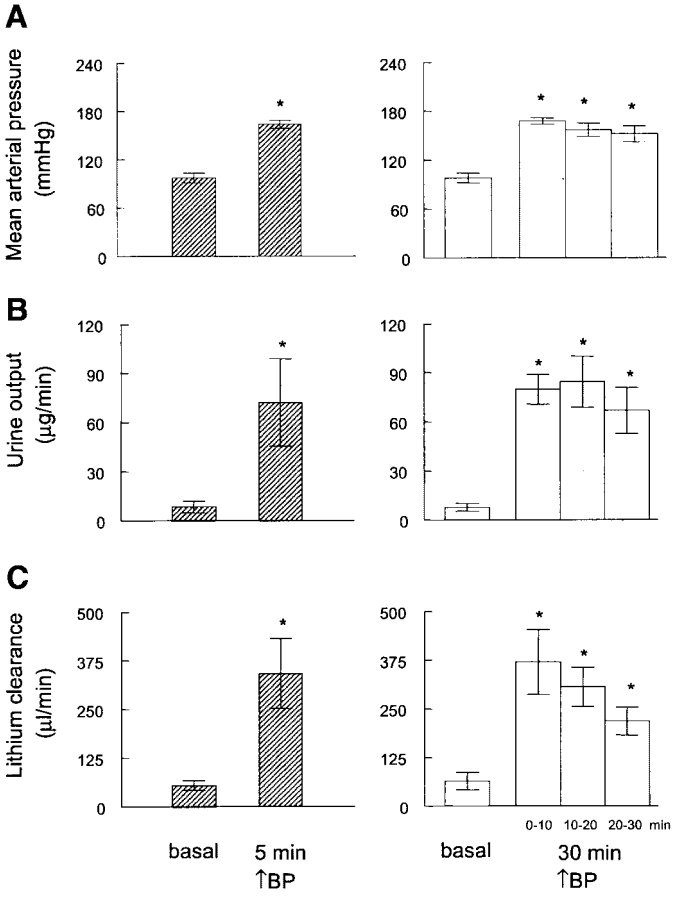

Fig. 4. Physiological responses to 5- and 30-min artery constriction. Summaries of groups studied after 5- (*left*) and 30-min hypertension (*right*) are shown. *A*: mean arterial pressure recorded from carotid artery. *B*: urine output collected over 5- or 10-min intervals, as indicated, expressed as urine weight (in μg/min). *C*: endogeneous lithium clearance (μl/min) calculated as urinary [Li^+] × urine output ÷ plasma [Li^+]. Values are means ± SE; $n = 5$ rats/group. * $P <$ 0.05 vs. basal period by paired Student's *t*-test.

apical NHE3, immunoblots of renal cortical fractions from control and 5- and 30-min hypertension protocols were probed with NHE3-C00. Figure 5*A* shows representative immunoblots, and Fig. 5*B* summarizes NHE3 redistribution in the three gradient windows, expressed as the percentage of the total. In controls, *WI* (enriched in apical membranes) contains 37 ± 4.15% of total NHE3 immunoreactivity. After 5-min acute hypertension, *WI* NHE3 is reduced from 37 ± 4.2 to 17 ± 7.9%, and after 30-min hypertension to 7.0 ± 1.8% of total NHE3. *WII* (apical and intermicrovillar cleft markers) increases from 54 ± 3.2 NHE3 to 73 ± 5.9 then to 72 ± 2.2% after 5- and 30-min hypertension, respectively. *WIII* (endosomal and lysosomal markers) contains 9 ± 1.1% NHE3 in controls, is unchanged after 5 min (10 ± 2.6%), then increases to 22 ± 3.8% after 30-min hypertension. The results are consistent with a two-step process of internalization during hypertension; that is, NHE3 rapidly migrates from the apical brush border to the intermicrovillar cleft and perhaps dense apical tubules and subsequently, after 5 min, is transferred to endosome and/or lysosome pools.

Immunocytochemistry evidence for NHE3 internalization during acute hypertension. Confocal immunofluorescence analysis of NHE3 redistribution in response to acute hypertension was conducted in tandem with subcellular fractionation analysis. The purpose was to establish whether NHE3 was present in subapical pools after acute hypertension. Double labeling was performed on cryosections harvested from control and hypertension-challenged kidneys. NHE3-C00/FITC-conjugated goat anti-rabbit secondary antibody was used to image NHE3, and monoclonal anti-villin/Alexa 568-conjugated goat anti-mouse secondary antibody was used to image villin, the actin-bundling protein found in the microvilli. We did not fix the kidneys by perfusing them with fixative because our experimental purpose was to maintain a defined perfusion pressure, the variable under study in this project. After 5-min acute hypertension (or a control 5-min period), kidneys were fixed in situ, as described in EXPERIMENTAL PROCEDURES, for another 20 min while baseline or elevated blood pressure was recorded. Thus the experimental time point is between 5 and 25 min. In control rats, the staining of NHE3 is restricted to the brush border, as evidenced by colocalization with staining for villin (Fig. 6, *top right*, arrowhead). During hypertension, NHE3

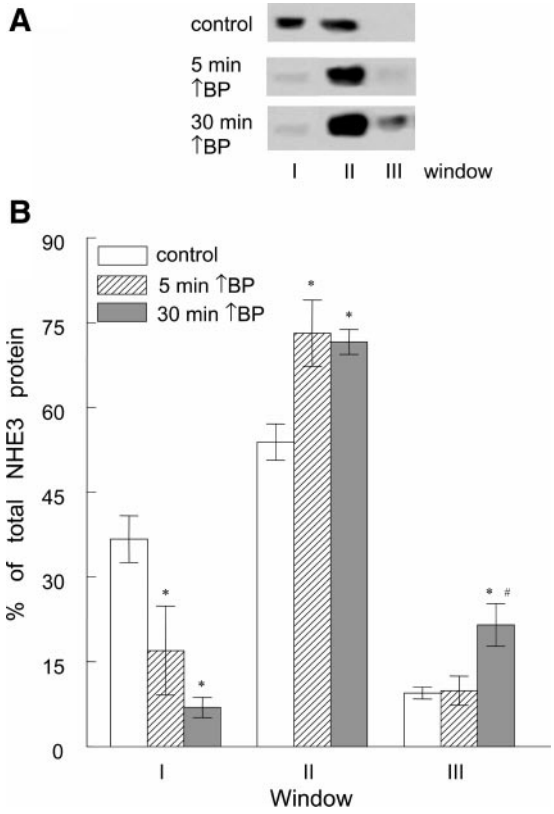

Fig. 5. Time course of NHE3 redistribution. *A*: representative NHE3 immunoblots of subcellular membrane windows of renal cortex from control rats and those studied after 5- and 30-min hypertension and probed with the polyclonal NHE3-C00 antibody. *B*: summary of NHE3 distribution in 3 windows expressed as the percentage of the total signal in all 3 windows for each time point. Values are means ± SE; $n = 4$ rats/group. *$P <$ 0.05 vs. control and #$P <$ 0.05 vs. 5-min hypertension by paired Student's *t*-test.

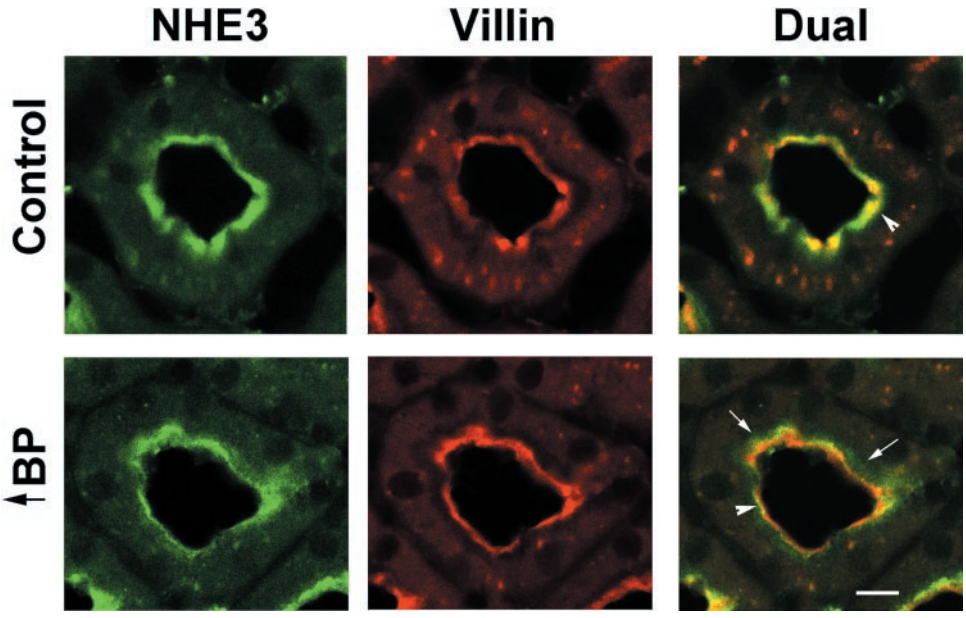

Fig. 6. Indirect immunofluorescence microscopy of NHE3 redistribution. NHE3 was detected in the proximal tubule in kidneys exposed to 25-min acute hypertension or paired sham treatment with in situ fixation with 2% paraformaldehyde, 75 mM lysine, and 10 mM Na-periodate during the last 20 min. Typical proximal tubules are shown from control (*top*) and acutely hypertensive (*bottom*) rats. Sections were doubly labeled with polyclonal anti-rabbit NHE3-C00 antibody, then FITC-conjugated anti-rabbit secondary antibody, and with monoclonal anti-villin antibody, then Alexa 568-conjugated anti-mouse secondary antibody. NHE3 staining is green (arrows), villin staining is red, and overlapping NHE3 and villin appears in yellow (arrowhead). Bar, 7 μm.

moves out of the apical brush-border microvilli, leaving the tops of the villi stained red with the anti-villin; NHE3 is detected in the intermicrovillar cleft region, where it coincides with villin (Fig. 6, *bottom*, yellow stain, arrowhead); and NHE3 appears in subapical vesicles, where it does not overlay villin (Fig. 6 *bottom*, green stain, arrow). These results provide visual correlation with the fractionation data demonstrating that the shift of NHE3 to heavier density fractions indicates a spatial redistribution out of the microvilli to intermicrovillar membranes and intracellular membranes.

Effect of acute hypertension on NHE3 activity. Although we demonstrated that acute hypertension provokes redistribution of proximal tubule NHE3 out of the apical microvilli to membranes with higher densities located below the microvilli, it is possible that this is not the key mechanism to inhibit proximal tubule Na^+ reabsorption. It is possible that internalization occurs secondarily or subsequent to inhibition of NHE3 transport activity. We next aimed to determine whether there was an accompanying inhibition of NHE3 activity/transporter during acute hypertension.

To establish that H^+ transport by the Na^+/H^+ exchangers can be measured by rates of quenching and reappearance of AO, the sensitivity of Na^+-dependent AO quenching to the NHE inhibitor amiloride was examined in the total S_o membranes. Na^+/H^+ exchange activity was measured by the initial rate of AO recovery in response to an inwardly directed Na^+ gradient expressed as fluorescence units per second per milligram protein. Ten microliters (250 μg) S_o membrane vesicles, loaded as described in EXPERIMENTAL PROCEDURES, were assayed as in Fig. 1. Figure 7 shows that the magnitude of AO quenching and recovery decreases as the amiloride concentration increases, with an apparent I_{50} of 100 μM in agreement with the published sensitivity of renal NHE3 (24).

Na^+/H^+ exchanger activity/protein was first measured in total renal cortex S_o membrane vesicles from

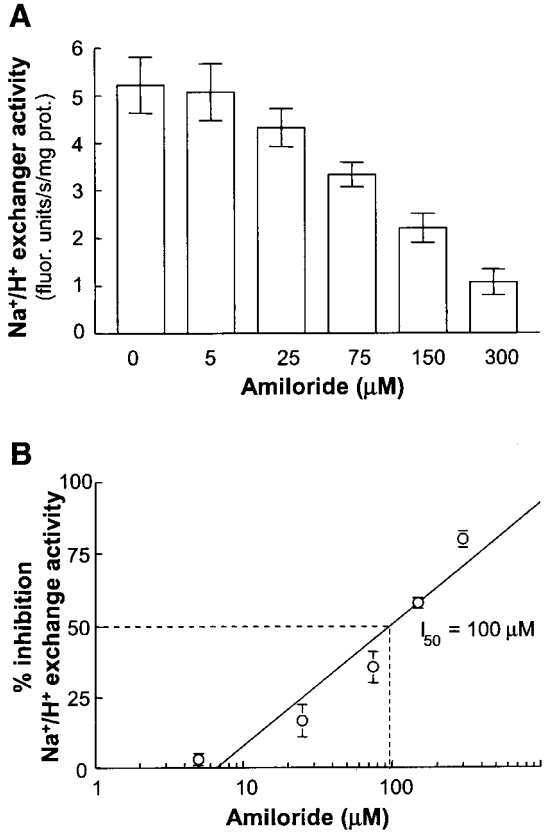

Fig. 7. Amiloride sensitivity of Na^+/H^+ exchanger activity. *A*: total cortex membrane vesicles were preloaded as described in Fig. 1 and then added to AO containing external buffer lacking Na^+ and containing the indicated concentrations of amiloride. Na^+/H^+ exchanger activity is expressed as the initial rate of AO fluorescence recovery after Na^+ addition. *B*: data in *A* plotted as %inhibition vs. log of amiloride concentration. I_{50} was obtained from intercept of dashed vertical line. fluor., Fluorescence; prot., protein. Values are means ± SE; $n = 3$ independent samples.

control and 30-min-hypertension-treated rats. Figure 8*A* shows that 30-min acute hypertension did not decrease total Na^+/H^+ exchanger activity in cortex membranes. Figure 8*B* shows that there was no change in NHE3 abundance when 5 and 10 μg of protein of the same samples were probed by immunoblot. These results indicate that the decrease in proximal tubule Na^+ transport after 30-min acute hypertension is not due to an inhibition of NHE3 activity or to a decrease in NHE3 protein pool size.

The constant Na^+/H^+ exchanger activity/NHE3 protein in S_o membranes during acute hypertension (Fig. 8) predicts that the shift in NHE3 protein from *WI* to *WII* and *WIII* (Figs. 3 and 5) will be paralleled by a shift in Na^+/H^+ exchanger transport activity from *WI* to *WII* and *WIII*. Na^+/H^+ exchanger activity and NHE3 protein levels were assayed in the same samples in controls and after 30-min hypertension and normalized to constant protein. Figure 9*A* demonstrates that there

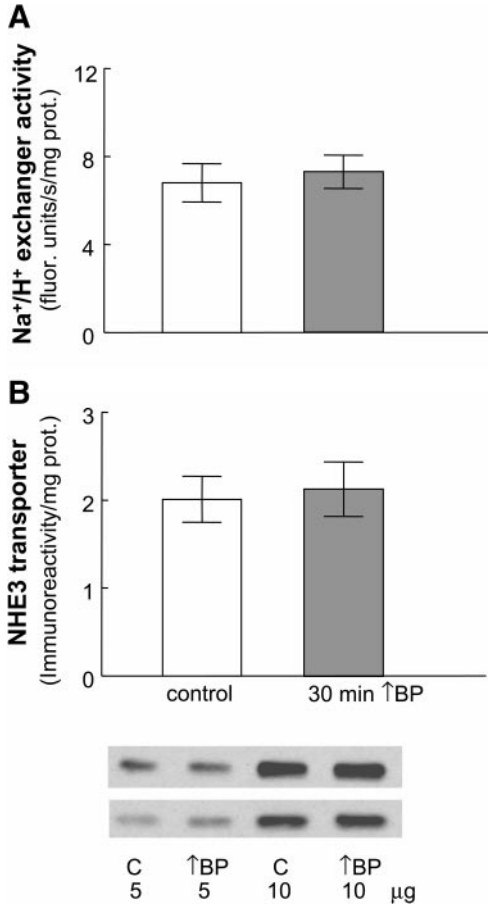

Fig. 8. Na^+/H^+ exchange activity and abundance in total cortical membranes. *A*: 250 μg of total cortex membrane vesicles (S_o) from control (C) or rats after 30-min hypertension were assayed for Na^+/H^+ exchanger transport activity as described in Figs. 1 and 7. The transport activity was a linear function of added protein (not shown). *B*: a constant amount of S_o protein was assayed for NHE3 abundance by immunoblotting with polyclonal anti-NHE3 L546 antibody, quantitated by scanning densitometry, and normalized to sample protein. Typical NHE3 immunoblots from 2 independent experiments are shown, in which the amount of protein assayed was in the linear range. Values are means ± SE; $n = 4$ rats/group.

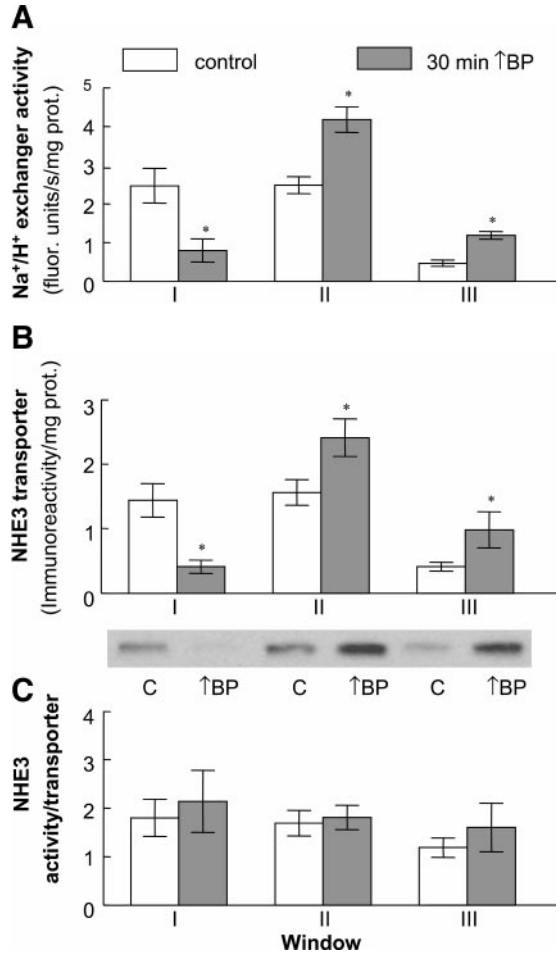

Fig. 9. Na^+/H^+ exchange activity and abundance in fractionated cortical membranes. *A*: Na^+/H^+ exchange activity was measured as the initial rate of AO recovery in 100-μg protein samples from the 3 membrane windows from control rats or those after 30-min hypertension. The amount of protein added was established to be in the linear range (not shown). *B*: NHE3 abundance was measured by immunoblot of a defined amount of protein from the 3 windows probed with polyclonal anti-NHE3 L546 antibody. NHE3 signals were quantitated by scanning densitometry and normalized to the amount of protein loaded. Representative immunoblots from control (C) and hypertension gradients (↑ BP) are shown. *C*: NHE3 activity/transporter was calculated by dividing the exchanger activity/protein by the NHE3 immunoreactivity signal/protein for each sample. Values are means ± SE; $n = 4$ rats/group. *$P < 0.05$ vs. corresponding control window by paired Student's *t*-test.

is a parallel shift in Na^+/H^+ exchanger activity: *WI*-specific activity decreased 68%, whereas *WII* activity increased 68% and *WIII* activity increased 153%. These changes paralleled the redistribution of NHE3 protein (Fig. 9*B*). Representative NHE3 immunoblots of samples from control (C) and acute hypertension (↑ BP) are included. Na^+/H^+ exchanger activity/NHE3 transporter for each sample is summarized in Fig. 9*C*. The results demonstrate that there is no detectable inhibition of Na^+/H^+ exchanger activity during acute hypertension. The appearance of Na^+/H^+ exchanger activity along with the NHE3 isoform indicates that the transport activity measured can be attributed to the NHE3 isoform. From these results, we conclude that the re-

duction in proximal tubule sodium transport during acute hypertension involves the trafficking of transport-competent Na^+/H^+ exchangers from apical membranes to subapical and endosomal/lysosomal membrane pools without inactivation.

DISCUSSION

This study provides three new findings concerning the molecular mechanisms responsible for inhibition of proximal tubule salt and water reabsorption during acute hypertension. First, NHE3 activity measured in response to in vivo acute hypertension, normalized to the NHE3 protein by quantitative immunoblot, did not decrease, providing evidence for redistribution of transport-competent NHE3 (Figs. 8 and 9). Second, improved confocal pictures provide clear evidence for retraction of NHE3 from the tops of the brush border and its appearance in subapical vesicles during acute hypertension (Fig. 6). Third, the time course study provides evidence for a two-step route for redistribution of NHE3 in response to acute hypertension: at 5 min, NHE3 leaves *WI*, enriched in apical brush-border markers, and moves to *WII*, enriched in the marker for intermicrovillar cleft and dense apical tubules found under the microvilli; then, at 30 min, the same percentage of NHE3 that left *WI* appears in *WIII*, enriched in the endosomal/lysosomal markers β-hexosaminidase and rab 5a. This redistribution coincides with increases in urine output and lithium clearance at 5 min of hypertension, evidence of decreased proximal sodium reabsorption. (Figs. 4 and 5). In addition, this study presents the characteristics of a new anti-NHE3 antibody that is better able to detect NHE3 in subapical and endosomal vesicles than other antibodies (Figs. 3 and 6).

The change in volume flow out of the proximal tubule during acute hypertension was estimated in this study from endogenous lithium clearance, which increased fivefold at 5 min and then fell to threefold over control at 30 min. Lithium clearance is a noninvasive measure of volume flow out of the proximal tubule determined by both the filtration rate (GFR) and the proximal reabsorption rate. In contrast, Chou and Marsh (9, 10) measured a progressive increase in volume flow from the proximal tubule (measured by videomicroscopy) of 18% as early as 1.5–2 min, which increased to 1.5-fold over baseline after 30 min of raising blood pressure 30–50 mmHg. The protocol in the present study may give a more rapid response of greater magnitude because blood pressure was increased 20–30 mmHg higher than in the Chou and Marsh studies. This higher blood pressure could lead to two differences: *1*) provide a bigger "signal" to inhibit proximal tubule Na^+ reabsorption (which was the motivation to raise the blood pressure further) and *2*) increase GFR. We didn't measure GFR in this study but we have done this routinely now and observed a transient increase during acute hypertension that returns to baseline within 15–20 min (not shown). The decrease in C_{Li^+} over this time course shown in Fig. 4 supports a transient in GFR; C_{Li^+} remains at threefold over control at 20–30 min, probably reflecting the inhibition of proximal reabsorption with a minimal increase in GFR. This magnitude is similar to what this laboratory has reported in related studies, and similar to what is observed when a carbonic anhydrase inhibitor is administered (32–34). Simlarly, using the same acute hypertension protocol used in our study, Yip et al. (31) recently measured NHE3 activity in situ as change in intracellular pH over time, measured noninvasively on the surface of the kidney, and found that apical membrane Na^+/H^+ exchanger activity was reduced to 0.59 ± 0.08 of baseline after 10 min of hypertension and remained at 0.48 ± 0.11 of baseline after 20 min of hypertension. That is, like the present study, the study by Yip et al. did not measure a significant progressive inhibition between 10 and 20 min, but a rapid and persistent decrease in Na^+ transport. These real time measurements of proximal tubule function cannot discriminate between removal of transport competent sodium transporters or inhibition of sodium transporters resident in the apical membrane. Our time course studies are enlightening in this regard as they demonstrate rapid removal of most of the NHE3 from the apical enriched membranes found in *WI* after only 5 min of acute hypertension, which persists through 30-min hypertension (Figs. 4 and 5). These results complement the in vitro study of Kurashima et al. (17) on the effect of phosphatidylinositol 3-kinase inhibition on NHE3 activity in NHE3-transfected Chinese hamster ovary cells. Most of the decrease in transport, loss of NHE3 from the cell surface, and accumulation of endocytic NHE3 occurred between 15 and 30 min after inhibition of phosphatidylinositol 3-kinase, which prevented the recycling and reinsertion of NHE3 back to the cell surface.

Yip et al. (30), using confocal microscopy, provided evidence that NHE3 is moved out of the microvilli during acute hypertension. However, because the proximal tubule has a rich array of vesicles immediately under the apical membrane, also referred to as dense apical tubules (DAT), it was difficult to discern internalization into endosomes vs. localization to the intermicrovillar clefts. To improve definition of the villi vs. subvilli membranes, we double labeled with NHE3 (FITC)- and villin (Alexa 568)-tagged antibodies. The results indicated that acute hypertension provokes a shift of NHE3 out of the microvilli, leaving red villin stain in the villi, to the intermicrovillar cleft region, where NHE3 colocalizes with villin (yellow stain), and the distinct appearance of NHE3 below the villi in subapical endosomes (green stain). These results agree with our previous fractionation study, which showed that villin distribution does not change during hypertension whereas NHE3 moves to the higher density regions coinciding with endosomal markers. Receptor internalization in the proximal tubule also occurs by a two-step process: using electron microscopy, Nielsen (23) demonstrated that insulin receptors first migrate laterally from the microvilli to the intermicrovillar

cleft region and are then internalized into endocytotic vacuoles and dense apical tubules.

There is extensive literature examining acute regulation of NHE3 activity in the proximal tubule by a variety of hormones including angiotensin II, endothelin, insulin, dopamine, and PTH (reviewed in Ref. 22). In reconstituted liposomes where trafficking is not a possibility, there is evidence for cAMP/PKA-mediated inhibition of Na^+/H^+ exchanger activity (27). In addition, we provided evidence that cAMP/PKA can mediate the removal of NHE3 from the plasma membrane: PTH (1–34), which couples to adenylate cyclase, decreases proximal tubule sodium reabsorption, and provokes NHE3 internalization whereas PTH (3–34), which does not couple to adenylate cyclase, does neither (34). These studies suggested the possibility that acute hypertension causes an inhibition of Na^+/H^+ exchanger activity followed by a retraction of NHE3 to the intermicrovillar cleft and then to the endosomes. We examined the hypothesis by measuring activity in total membranes isolated rapidly from pressure-challenged kidneys and in membranes fractionated to separate apical, intermicrovillar cleft, and endosomal enriched membranes. Because our previous studies demonstrated that enzymatic changes in basolateral Na,K-ATPase and apical alkaline phosphatase activity during acute hypertension persist through membrane fractionation (32, 33), we expected that changes in NHE3 activity resulting from covalent modification to persist as well. Na^+/H^+ exchanger transport activity was measured with an AO quenching technique. Although fluorescence-quenching techniques applied in living cells are usually considered as semiquantitative (16), we optimized the method for quantitation: *1*) established a linear range for membrane protein addition vs. initial rate of AO fluorescence recovery at 6 μM AO and <250 μg of added protein for total membranes and 100 μg for membrane fractions; and *2*) established that the concentration of amiloride that inhibited exchanger activity 50% (I_{50}) was 100 μM, as reported for NHE3, which is much lower than that for NHE1 and NHE2, where $I_{50} \approx 3$ μM (11, 24). In fact, there was no discernable decrease in Na^+/H^+ exchanger activity with 5 μM amiloride, indicating that NHE3 is the predominant Na^+/H^+ exchanger in the renal cortex, as we have previously established at the mRNA level (1). H^+-ATPase in the membrane vesicles does not contribute to the Na^+-dependent pH change measured in the assay because H-ATPase activity is Na^+ independent, and no ATP was added to the assay. Also critical for quantitation, immunoblots were established to be in the linear range for membrane protein addition vs. autoradiographic density of NHE3 within each window, necessary for calculation of transport activity/transport protein.

The assay of Na^+/H^+ exchanger activity/NHE3 protein in total membranes indicated both no change in total pool size of NHE3 and no change in activity per transporter. The assays in fractionated membranes revealed that the decrease in exchanger activity in apical membranes (*WI*) can be accounted for by NHE3 removal, that the increase in activity in intermicrovillar cleft and endosomes (*WII* and *WIII*) can be accounted for by NHE3 addition to these higher density membranes and that these redistributed exchangers are as active as those measured in control apical membranes. We conclude that the decrease in Na^+ transport during acute hypertension does not involve the inhibition or degradation of transporter but internalization of NHE3 from brush border to subapical stores.

In another study comparing changes in NHE3 activity and abundance in proximal tubule brush-border vesicles, Moe and colleagues (13) gave a bolus of PTH to parathyroidectomized rats and measured a 14% fall in transport activity at as early as 30 min, which preceded a statistically significant 33% disappearance of NHE3 protein from the brush-border membranes 4 h after PTH administration. The authors conclude that NHE3 activity is rapidly decreased before NHE3 is internalized at 4 h. Because these are small changes, another plausible interpretation is that there was a gradual internalization of NHE3 protein that paralleled the decrease in activity but it couldn't be statistically established that the pH-driven $^{22}Na^+$ flux measurement of NHE3 transport activity can detect smaller changes than the enhanced chemiluminesence-based antibody-antigen measurement of NHE3 protein. Specifically, these investigators focused on comparing loss of activity to the loss of NHE3 protein from a brush-border fraction: at 2 h after PTH administration, they report a 28% decrease in activity and a 12% (nonsignificant) decrease in NHE3 protein, which translates into a 16% decrease in activity/transport in the apical membranes, and by 4 h all of the change in activity can be accounted for by a loss of NHE3 protein. The advantage of the approach used in our present study was that we analyzed total membranes where we could compare loss of NHE3 activity and transport from the apical pool to gain of NHE3 activity and transport in intramicrovillar and endosomal membranes.

Na^+/H^+ exchangers have been previously detected in intracellular vesicles in the proximal tubule, and their activity has been assessed with mixed results. Sabolic and Brown (26) detected Na^+/H^+ exchange activity, sensitive to intravesicular amiloride, in vesicles from rat renal cortex using AO quenching, and D'Souza et al. (12) detected NHE3 accumulation and transport activity in recycling endosomes in exchanger-deficient activator protein (AP)-1 cells transfected with NHE3. In contrast, Biemesderfer et al. (2) fractionated rabbit renal brush border and concluded that NHE3 exists in two oligomeric states: an active 9.6-S form present in brush-border microvilli prepared by divalent cation precipitation and an inactive 21-S megalin-associated NHE3 in dense vesicles containing markers of the intermicrovillar cleft collected from OptiPrep density gradients. Can we reconcile these findings with those in this present study? There are clear differences between the brush-border (active) vs. OptiPrep (inactive) membrane preparations assayed in the Biemesderfer study, and both are different from the membranes assayed in this study, where total

membranes are all resolved on the same sorbitol gradient into apical, intermicrovillar cleft, and endosomal membrane pools and assayed in parallel. One possible interpretation is that NHE3 exchanger activity is transiently inactivated during NHE3 internalization when NHE3 moves to the cleft and associates with megalin, followed by reactivation of NHE3 as it entered in the subapical vesicles and endosomes. However, because Na^+/H^+ exchanger activity/NHE3 protein was not different between *WI* and *WII* in controls or after 30-min hypertension, a corollary to this interpretation would be that there is only a very small fraction of megalin-associated inactivated NHE3 in *WII*. Another line of investigation suggests that NHE3 is not only active during internalization but that activity is critical to the early phase of apical endocytosis. In a proximal tubule cell line, Gekle and colleagues (15) demonstrated that NHE3 inhibition rapidly blocks internalization of prebound albumin and attenuated degradation of internalized albumin without changing general protein degradation or internalization of transferrin from the basolateral membrane.

The present study shows that sodium transport can be rapidly decreased in the proximal tubule by retracting active NHE3 from the apical membrane. We previously established that redistribution of NHE3 is a reversible response: when blood pressure is restored to basal levels after acute hypertension, NHE3 returns to its original distribution pattern in the sorbitol gradient, and sodium transport in the proximal tubule is restored (32). There would be physiological advantages to maintaining NHE3 activity during the internalization that accompanies acute hypertension: NHE3 activity could contribute to both endocytosis and endosomal acidification, and transporters would be active when returned to the apical membrane after blood pressure is restored.

We are grateful to Austin Mircheff and Richard Lubman for guidance with the transport methods and to Michaela Mac Veigh for skillful assistance in confocal microscopy.

This work was supported by National Institute of Diabetes and Digestive and Kidney Diseases Grant DK-34316, fellowship support to L. Yang and P. K. K. Leong from the American Heart Association, Western States Affiliate, and National Institutes of Health Core Center Grant DK-48522.

REFERENCES

1. **Azuma KK, Balkovetz DF, Magyar CE, Lescale-Matys L, Zhang YB, Chambrey R, Warnock DG, and McDonough AA.** Renal Na^+/H^+ exchanger isoforms and their regulation by thyroid hormone. *Am J Physiol Cell Physiol* 270: C585–C592, 1996.
2. **Biemesderfer D, DeGray B, and Aronson PS.** Active (9.6 s) and inactive (21 s) oligomers of NHE3 in microdomains of the renal brush border. *J Biol Chem* 276: 10161–10167, 2001.
3. **Biemesderfer D, Dekan G, Aronson PS, and Farquhar MG.** Biosynthesis of the gp330/44-kDa Heymann nephritis antigenic complex: assembly takes place in the ER. *Am J Physiol Renal Fluid Electrolyte Physiol* 264: F1011–F1020, 1993.
4. **Biemesderfer D, Pizzonia J, Abu-Alfa A, Exner M, Reilly R, Igarashi P, and Aronson PS.** NHE3: a Na^+/H^+ exchanger isoform of renal brush border. *Am J Physiol Renal Fluid Electrolyte Physiol* 265: F736–F742, 1993.
5. **Briggs JP and Schnermann JB.** Whys and wherefores of juxtaglomerular apparatus function. *Kidney Int* 49: 1724–1726, 1996.
6. **Brown D, Lydon J, McLaughlin M, Stuart-Tilley A, Tyszkowski R, and Alper S.** Antigen retrieval in cryostat tissue sections and cultured cells by treatment with sodium dodecyl sulfate (SDS). *Histochem Cell Biol* 105: 261–267, 1996.
7. **Bucci C, Wandinger-Ness A, Lutcke A, Chiariello M, Bruni CB, and Zerial M.** Rab5a is a common component of the apical and basolateral endocytic machinery in polarized epithelial cells. *Proc Natl Acad Sci USA* 91: 5061–5065, 1994.
8. **Chibalin AV, Ogimoto G, Pedemonte CH, Pressley TA, Katz AI, Feraille E, Berggren PO, and Bertorello AM.** Dopamine-induced endocytosis of Na^+,K^+-ATPase is initiated by phosphorylation of Ser-18 in the rat alpha subunit and is responsible for the decreased activity in epithelial cells. *J Biol Chem* 274: 1920–1927, 1999.
9. **Chou CL and Marsh DJ.** Time course of proximal tubule response to acute hypertension in the rat. *Am J Physiol Renal Fluid Electrolyte Physiol* 254: F601–F607, 1988.
10. **Chou CL and Marsh DJ.** Role of proximal convoluted tubule in pressure diuresis in the rat. *Am J Physiol Renal Fluid Electrolyte Physiol* 251: F283–F289, 1986.
11. **Counillon L and Pouyssegur J.** The expanding family of eucaryotic Na(+)/H(+) exchangers. *J Biol Chem* 275: 1–4, 2000.
12. **D'Souza S, Garcia-Cabado A, Yu F, Teter K, Lukacs G, Skorecki K, Moore HP, Orlowski J, and Grinstein S.** The epithelial sodium-hydrogen antiporter Na^+/H^+ exchanger 3 accumulates and is functional in recycling endosomes. *J Biol Chem* 273: 2035–2043, 1998.
13. **Fan L, Wiederkehr MR, Collazo R, Wang H, Crowder LA, and Moe OW.** Dual mechanisms of regulation of Na/H exchanger NHE3 by parathyroid hormone in rat kidney. *J Biol Chem* 274: 11289–11295, 1999.
14. **Fernandez-Llama P, Andrews P, Ecelbarger CA, Nielsen S, and Knepper M.** Concentrating defect in experimental nephrotic syndrone: altered expression of aquaporins and thick ascending limb Na+ transporters. *Kidney Int* 54: 170–179, 1998.
15. **Gekle M, Freudinger R, and Mildenberger S.** Inhibition of Na+-H+ exchanger-3 interferes with apical receptor-mediated endocytosis via vesicle fusion. *J Physiol (Lond)* 531: 619–629, 2001.
16. **Kotyk A and Slavik J.** *Intracellular pH and Its Measurement.* Boca Raton, FL: CRC, 1989, p.56.
17. **Kurashima K, Szabo EZ, Lukacs G, Orlowski J, and Grinstein S.** Endosomal recycling of the Na^+/H^+ exchanger NHE3 isoform is regulated by the phosphatidylinositol 3-kinase pathway. *J Biol Chem* 273: 20828–20836, 1998.
18. **Laemmli UK.** Cleavage of structural proteins during the assembly of the head of bacteriophage T4. *Nature* 227: 680–685, 1970.
19. **Lotscher M, Scarpetta Y, Levi M, Halaihel N, Wang H, Zajicek HK, Biber J, Murer H, and Kaissling B.** Rapid downregulation of rat renal Na/P_i cotransporter in response to parathyroid hormone involves microtubule rearrangement. *J Clin Invest* 104: 483–494, 1999.
20. **Lowry OH, Rosebrough NJ, Farr AL, and Randall RJ.** Protein measurement with the Folin phenol reagent. *J Biol Chem* 193: 265–275, 1951.
21. **Magyar CE and McDonough AA.** Molecular mechanisms of sodium transport inhibition in proximal tubule during acute hypertension. *Curr Opin Nephrol Hypertens* 9: 149–156, 2000.
22. **Moe OW.** Acute regulation of proximal tubule apical membrane Na/H exchanger NHE3: role of phosphorylation, protein trafficking, and regulatory factors. *J Am Soc Nephrol* 10: 2412–2425, 1999.
23. **Nielsen S.** Endocytosis in proximal tubule cells involves a two-phase membrane-recycling pathway. *Am J Physiol Cell Physiol* 264: C823–C835, 1993.
24. **Noël J and Pouyssëgur J.** Hormonal regulation, pharmacology, and membrane sorting of vertebrate Na^+/H^+ exchanger isoforms. *Am J Physiol Cell Physiol* 268: C283–C296, 1995.
25. **Reenstra WW, Warnock DG, Yee VJ, and Forte JG.** Proton gradients in renal cortex brush-border membrane vesicles. *J Bio Chem* 256: 11663–11666, 1981.

26. **Sabolic I and Brown D.** Na^+ (Li^+)-H^+ exchange in rat renal cortical vesicles with endosomal characteristics. *Am J Physiol Renal Fluid Electrolyte Physiol* 258: F1245–F1253, 1990.
27. **Shenolikar S and Weinman EJ.** NHERF: targeting and trafficking membrane proteins. *Am J Physiol Renal Physiol* 280: F389–F395, 2001.
28. **Thomsen K.** Lithium clearance: a new method for determining proximal and distal tubular reabsorption of sodium and water. *Nephron* 37: 217–223, 1984.
29. **Warnock DG, Reenstra WW, and Yee VJ.** Na^+/H^+ antiporter of brush border vesicles: studies with acridine orange uptake. *Am J Physiol Renal Fluid Electrolyte Physiol* 242: F733–F739, 1982.
30. **Yip KP, Tse CM, McDonough AA, and Marsh DJ.** Redistribution of Na^+/H^+ exchanger isoform NHE3 proximal tubules induced by acute and chronic hypertension. *Am J Physiol Renal Physiol* 275: F565–F575, 1998.
31. **Yip KP, Wagner AJ, and Marsh DJ.** Detection of apical Na^+/H^+ exchanger activity inhibition in proximal tubules induced by acute hypertension. *Am J Physiol Regulatory Integrative Comp Physiol* 279: R1412–R1418, 2000.
32. **Zhang YB, Magyar CE, Norian JM, Holstein-Rathlou N-H, Mircheff AK, and McDonough AA.** Reversible effects of acute hypertension on proximal tubule sodium transporters. *Am J Physiol Cell Physiol* 274: C1090–C1100, 1998.
33. **Zhang YB, Mircheff AK, Hensley CB, Magyar CE, Warnock DG, Chambrey R, Yip KP, Marsh DJ, Holstein-Rathlou N-H, and McDonough AA.** Rapid redistribution and inhibition of renal sodium transporters during acute pressure natriuresis. *Am J Physiol Renal Fluid Electrolyte Physiol* 270: F1004–F1014, 1996.
34. **Zhang YB, Norian JM, Magyar CE, Holstein-Rathlou N-H, Mircheff AK, and McDonough AA.** In vivo PTH provokes apical NHE3 and NaPi2 redistribution and Na-K-ATPase inhibition. *Am J Physiol Renal Physiol* 276: F711–F719, 1999.